Rendiconti di Matematica, Serie VII
Volume 25, Roma (2005), 33-52

Matrix-free numerical torus bifurcation of periodic orbits

EUGENE ALLGOWER – ULF GARBOTZ – KURT GEORG†

Abstract: *We consider systems*

$$\dot{\varphi} = f(\varphi, \lambda)$$

where $f : \mathbb{R}^n \times \mathbb{R} \to \mathbb{R}^n$. Such systems often arise from space discretizations of parabolic PDEs. We are interested in branches (with respect to λ) of periodic solutions of such systems.

In the present paper we describe a numerical continuation method for tracing such branches. Our methods are matrix-free, i.e., Jacobians are only implemented as actions, this enables us to allow for large n. Of particular interest is the detection and precise numerical approximation of bifurcation points along such branches: especially period-doubling and torus bifurcation points. This will also be done in a matrix-free context combining Arnoldi iterations (to obtain coarse information) with the calculation of suitable test functions (for precise approximations). We illustrate the method with the one- and two-dimensional Brusselator.

1 – Introduction

Recently, Georg [5] discussed a general setting for performing numerical continuation in a matrix-free setting. Transpose-free iterative linear solvers (see, e.g., [15]) can be effectively incorporated into such large-scale problems. A frequent application of numerical continuation concerns the detection of singularities and bifurcation points on a solution branch. By means of suitable test

Key Words and Phrases: *Matrix-free continuation – Numerical bifurcation – Torus bifurcation.*
A.M.S. Classification: 65P30 – 37M20 – 37G15

functions various bifurcation points can also be detected and approximated in a matrix free setting.

In this paper we describe how to numerically trace periodic orbits in a matrix-free way. We also present a test function for detecting and approximating torus bifurcations in a matrix-free setting. Numerical results for torus bifucation arising in the Brusselator equations in one and two dimensions are given.

The results reproduce the branches computed in [12], [13], where the Newton-Picard Gauss Seidel method was used. The test functions derived here to characterize bifurcations were used to obtain highly accurate approximations of the bifurcation points.

In order to describe the numerical tracing for the problems considered here, we review several of the ideas in [5].

2 – The Problem Setting

We consider systems

$$\dot{\varphi} = f(\varphi, \lambda) \tag{1}$$

where $f : \mathbb{R}^n \times \mathbb{R} \to \mathbb{R}^n$. Such systems often arise from space discretizations of parabolic PDEs. We are interested in branches (with respect to λ) of periodic solutions of such systems.

We denote a solution of (1) which has initial value u for $t = 0$ with $\varphi(u, t, \lambda)$. We have that $t \mapsto \varphi(u, t, \lambda)$ is periodic with period T iff

$$\varphi(u, T, \lambda) - u = 0. \tag{2}$$

However, even fixing λ, all points u of the same periodic orbit would satisfy this equation, hence we need an additional *phase condition*, say

$$h(u, T, \lambda) = 0 \tag{3}$$

to single out, at least locally, one point per orbit (see, e.g., [16]). In our numerical example we used the Poincaré phase condition

$$(u - \hat{u})^T f(\hat{u}, \lambda) = 0 \tag{4}$$

where $\hat{u}$ is some current point close to some orbit for given λ. This point will, of course, need to be adapted regularly. Let us remark that the Poincaré phase condition has proven to be an effective choice, see [12], [13].

Let us form the equation

$$H(u, T, \lambda) := \begin{bmatrix} \varphi(u, T, \lambda) - u \\ h(u, T, \lambda) \end{bmatrix} = 0. \tag{5}$$

For almost all choices of λ there is a neighbourhood of the orbit such that 0 is a regular value of H, if $\hat{u}$ is in that neigbourhood.

Hence, the periodic orbits of (1) can be traced by using numerical continuation methods (arising from varying λ) on equation (5). In particular, a matrix-free approach is very suitable if we are interested in allowing large dimensions n, since an action of the (full) Jacobian H' can be readily obtained, as we will see in Section 8. On the other hand, an explicit evaluation of the full Jacobian for large n is prohibitively expensive (see, e.g., [12], [13]). Hence, in this case direct linear solving methods are generally out of the question.

A numerical continuation method traces the solution branches of $H^{-1}(0)$. The method is called *matrix-free* if the Jacobian of H is not calculated explicitly, but only its action on a vector is given via some efficient process. In connection with modern (transpose-free) iterative linear solvers, see, e.g., [15], this is often a suitable approach for large systems, in particular for those investigated here.

Our main interest will center on the precise numerical detection of bifurcation points along solution branches of $H^{-1}(0)$. These special points on a solution branch are characterized by an additional equation

$$\tau(u, T, \lambda) = 0$$

where $\tau : \mathbb{R}^n \times \mathbb{R} \times \mathbb{R} \to \mathbb{R}$ can be viewed as a so-called *test function*. Note that also the detection and approximation of bifurcation points is carried out here in a matrix-free context.

Let us briefly describe the different bifurcation scenarios we are interested in for the periodic solutions of the dynamical system (1). Here is a list, see also [16]:

1. We briefly mention the case of a simple bifurcation point. This case, however, is documented rather well in the literature.
2. A singularity which displays a characteristic feature of periodic solutions is a period-doubling bifurcation. It turns out that the approach is rather similar to the simple bifurcation.
3. The most intriguing bifurcation is a torus bifurcation, which is a bit similar to Hopf bifurcation (and is sometimes also called a Hopf bifurcation of limit cycles). This will be our main topic.

3 – Numerical Continuation

We consider the numerical tracing of a solution branch

$$s \mapsto (u(s), T(s), \lambda(s))$$

of Equation (5). For simplicity, we view s as an arc-length parameter. Numerically, we actually perform pseudo-arclength steps, see, e.g., [1], [8].

A numerical continuation (predictor-corrector) method repeats two steps:

1. A predictor step generates an approximate point further along the solution curve, typically by linear extrapolation.
2. A corrector step finds a point approximately on the solution curve and close to the predicted point, typically by Newton-like steps.

The following algorithm sketches a possible implementation of this idea. For a more compact notation, we use $x := (u, T, \lambda) \in \mathbb{R}^{n+2}$, $\tilde{x} := (\tilde{u}, \tilde{T}, \tilde{\lambda}) \in \mathbb{R}^{n+2}$.

– **Algorithm 6 (Matrix-Free Predictor-Corrector)**

1. **Initialization**
   choose x such that $H(x) \approx 0$
   choose approximate tangent S such that $H'(x)S \approx 0$, $||S|| = 1$
   choose step size $h > 0$
   choose small reduction factor $1 \gg \eta > 0$
2. repeat
   (a) **Predictor**
   $\tilde{x} \leftarrow x + hS$
   (b) **Corrector**
   find Δx such that

$$\left\| \begin{bmatrix} H(\tilde{x}) \\ 0 \end{bmatrix} + \begin{bmatrix} H'(\tilde{x}) \\ S^T \end{bmatrix} \Delta x \right\| \leq \eta \left\| \begin{bmatrix} H(\tilde{x}) \\ 0 \end{bmatrix} \right\|$$

   via a transpose-free iterative linear solver, see, e.g., [15]
   $\tilde{x} \leftarrow \tilde{x} + \Delta x$
   (c) determine new h
   $S \leftarrow (\tilde{x} - x)/||\tilde{x} - x||$
   $x \leftarrow \tilde{x}$

Remark 7. The corrector step approximately solves

$$\begin{bmatrix} H(x) \\ S^T(x - \tilde{x}) \end{bmatrix} = 0$$

for x using an inexact Newton step. In our numerical examples, we use several such Newton steps in fact while reducing η.

4 – Calculating Special Points

When tracing a solution branch

$$s \mapsto (u(s), T(s), \lambda(s)) =: x(s)$$

of (5), one is often interested in special points on this branch. They can be of various types. Our cases of interest are covered by requiring that a certain test function $\tau : \mathbb{R}^{n+2} \to \mathbb{R}$ changes sign. Hence we seek a point $x^* \in \mathbb{R}^{n+2}$ such that

$$\begin{bmatrix} H(x^*) \\ \tau(x^*) \end{bmatrix} = 0 \ . \tag{8}$$

The following Lemma is easy to see:

LEMMA 9. *Let $x^* = x(s^*)$ be a regular zero point of H, i.e., the Jacobian $H'(x^*)$ has maximal rank. Then the following statements are equivalent:*

1. *$\tau(x(s))$ has a simple zero at $s = s^*$.*
2. *x^* is a regular zero point of* (8).

Once an approximation of x^* is found, we could, of course, use an inexact Newton's method directly on (8) to obtain a better approximation, i.e., without continuing to follow a path. Note, however, that this places a calculation of τ into the innermost loop of the method, i.e., while evaluating the functions in (8).

In the context of bifurcation analysis an evaluation of τ may be rather costly, e.g., in the case of torus bifurcation, see Theorem 13 below. Therefore, in our path following context, we use a somewhat different approach, which places an evaluation of τ into the outermost loop: During the numerical continuation, we monitor the sign of τ. Assume that a situation $\tau(x_-)\tau(x_+) < 0$ is encountered for two subsequent points x_-, x_+ on the solution curve. Then we introduce the approximate tangent

$$S := (x_+ - x_-)/||x_+ - x_-||$$

and the linear approximations

$$p(s) = x_- + s\, S \approx x(s)$$

Now let $q(s)$ be the solution of

$$\begin{bmatrix} H(q) \\ S^T(q - p(s)) \end{bmatrix} = 0 \ .$$

Hence, $q(s)$ can be viewed as the corrector-point to the predictor point $p(s)$. Clearly, $q(s)$ can be approximated via an iterative nonlinear solver using a

matrix-free double loop, the outer loop consisting of a Newton iteration, and the inner loop being a transpose-free iterative linear solver. We now find a zero of the function $s \mapsto \tau(q(s))$ via a secant-like method (e.g., Brent's Method, see [2]).

The resulting method for calculating x^* is implemented as a matrix-free triple loop, the outer loop being the secant-like method. Note, however, that the iterative methods representing the two inner loops can be started with increasingly improved values. Alternatively, a modification of this approach can be implemented into the numerical continuation method as a steplength strategy, see [1, Section 8.1] for details. This modification permits a matrix-free implementation consisting of a double loop.

We will apply these ideas to test functions τ that signal certain types of bifurcation points.

5 – Simple Bifurcation Points

Bordered matrices are an important tool for a numerical unfolding of singularities. For example, this is one of the principal themes of the book [6]. A consequence of [6, Proposition 3.2.1] is Keller's Lemma, see [8]:

Let $A \in \mathbb{R}^{n\times n}$ have rank $n-k$, and let $B, C \in \mathbb{R}^{n\times k}$. Then

$$\begin{bmatrix} A & B \\ C^T & 0 \end{bmatrix}$$

is nonsingular if and only if

$$[\, A \quad B \,] \text{ and } \begin{bmatrix} A \\ C^T \end{bmatrix}$$

have full rank. Since the set of invertible matrices is open in the space of square matrices, the choice of matrices B, C such that the above matrices have full rank is usually easy to fulfill. However, for numerical purposes, one needs to take issues of condition into account, see Remark 20.

The following is a well-known fact, see, e.g., [5], [6]. A simple bifurcation point $x^* = x(s^*)$ is characterized by the fact that the determinant

$$\det \begin{bmatrix} H'(x(s)) \\ S^T \end{bmatrix}$$

changes sign at $s = s^*$. Here S has to be some approximate tangent, i.e., $S \approx \dot{x}(s^*)$. However, this is not a numerically suitable choice of a test function. A better choice is to consider the following bordered system:

$$\begin{bmatrix} \begin{bmatrix} H'(x(s)) \\ S^T \end{bmatrix} & a \\ b^T & 0 \end{bmatrix} \begin{bmatrix} \xi(s) \\ \tau(s) \end{bmatrix} = \begin{bmatrix} 0 \\ 1 \end{bmatrix}$$

If $a, b \in \mathbb{R}^{n+2}$ are chosen such that

$$\begin{bmatrix} \begin{bmatrix} H'(x(s^*)) \\ S^T \end{bmatrix} & a \end{bmatrix} \text{ and } \begin{bmatrix} \begin{bmatrix} H'(x(s^*)) \\ S^T \end{bmatrix} \\ b^T \end{bmatrix}$$

have full rank, then the matrix of the bordered system is non-singular for $s \approx s^*$ where $x^* = x(s^*)$ is a simple bifurcation point. It is easy to see (e.g., via Cramer's Rule) that τ is a test-function for the simple bifurcation point x^*, i.e., τ has a simple zero at $s = s^*$.

Hence, in principle, we could use the method described in Section 4 to detect and approximate simple bifurcation points. However, the approximation cannot be executed very accurately since the Jacobian

$$\begin{bmatrix} H'(x(s)) \\ S^T \end{bmatrix}$$

becomes singular at $s = s^*$, and hence the numerical tracing of $x(s)$ becomes unstable for $s \approx s^*$. It is, however, possible to obtain a matrix-free stable method, see [5].

6 – Period-Doubling Bifurcation

If u is a T-periodic orbit of (1), i.e., $H(u, T, \lambda) = 0$, then $\partial_1\varphi(u, T, \lambda)$ is called the monodromy matrix. A simple period-doubling bifurcation point $x^* = (u^*, T^*, \lambda^*)$ is characterized in the following way, see, e.g., [16]: For an algebraically simple real eigenvalue $\nu(s)$ of $s \mapsto \partial_1\varphi(u(s), T(s), \lambda(s))$ there holds $\nu(s^*) = -1$ and $\nu'(s^*) \neq 0$. Note that this implies that the determinant of

$$\partial_1\varphi\big(u(s), T(s), \lambda(s)\big) + \mathrm{I}$$

changes sign at $s = s^*$.

In analogy to Section 5 we obtain the following numerical test function for detecting such a point while numerically following the curve $s \mapsto x(s)$.

THEOREM 10. *Let $x^* = x(s^*)$ be a simple period-doubling bifurcation point as defined above. Suppose $b, c \in \mathbb{R}^n$ are chosen such that the bordered matrix in the following system is invertible*

$$\begin{bmatrix} \partial_1\varphi\big(u(s), T(s), \lambda(s)\big) + \mathrm{I} & b \\ c^T & 0 \end{bmatrix} \begin{bmatrix} \xi(s) \\ \tau(s) \end{bmatrix} = \begin{bmatrix} 0 \\ 1 \end{bmatrix}. \tag{11}$$

Then the system is non-singular for $s \approx s^*$, and $\tau(s)$ has a simple zero at $s = s^*$.

Contrary to a simple bifurcation point, however, a simple period-doubling bifurcation point is not a singular point on the curve $H^{-1}(0)$, and hence the method described in Section 4 applies. The only additional complexity of the problem comes from the calculation of τ which requires one matrix-free loop.

7 – Torus bifurcation

We consider again a local (i.e., for $s \approx s^*$) parametrization $s \mapsto (u(s),T(s),\lambda(s))$ of $H^{-1}(0)$, and define the monodromy matrix $A(s) := \partial_1 \varphi\big(u(s), T(s), \lambda(s)\big)$. A simple torus bifurcation point

$$(u^*, T^*, \lambda^*) = (u(s^*), T(s^*), \lambda(s^*))$$

is characterized in the following way, see, e.g., [6], [10], [16]: Let $\nu(s) + i\omega(s)$ be an algebraically simple complex eigenvalue of $A(s)$ for $s \approx s^*$. Hence

$$A(s)(v_1(s) + iv_2(s)) = (\nu(s) + i\omega(s))(v_1(s) + iv_2(s))$$

for linearly independent $v_1(s), v_2(s) \in \mathbb{R}^n$. Let the two eigenvalues furthermore cross the unit circle in the sense that

$$\epsilon(s) := \nu(s)^2 + \omega(s)^2 - 1$$

has a simple zero at $s = s^*$ with $\omega(s^*) \neq 0$. It follows that

$$(A - \nu)v_1 = -\omega v_2 \ ,$$

$$(A - \nu)v_2 = \omega v_1 \ .$$

Hence, if we consider the real vector space

$$E(s) = \operatorname{span}\{\, v_1(s), v_2(s) \,\},$$

then the kernel of

$$(A(s) - \nu(s)\ \mathrm{I})^2 + \omega(s)^2\ \mathrm{I} = A(s)^2 - 2\nu(s)A(s) + \ \mathrm{I} + \epsilon(s)\ \mathrm{I}$$

is $E(s)$. Also note that the two-dimensional space $E(s)$ is invariant under $A(s)$, and that $A(s)$ is bijective on $E(s)$ for $s \approx s^*$ since its two eigenvalues are close to the unit circle.

The following theorem describes a test function for a simple torus bifurcation point which we have implemented numerically. The introduction of the system (14) below was motivated by similar systems for Hopf bifurcation, such as [3], [17].

For the proof of the theorem we introduce the following notation:

DEFINITION 12. For $f, g : \mathbb{R}^{k_1} \to \mathbb{R}^{k_2}$ we define $f(z) \succ g(z)$ if there is an $\epsilon > 0$ such that $||f(z)|| \geq \epsilon ||g(z)||$ for sufficiently small $||z||$.

THEOREM 13. *Let $(u(s^*), T(s^*), \lambda(s^*))$ be a simple torus bifurcation point as described above. Assume that $c, d \in \mathbb{R}^n$ are chosen so that*

$$\begin{bmatrix} A(s^*)^2 - 2\nu(s^*)A(s^*) + \mathrm{I} \\ c^T \\ d^T \end{bmatrix} \text{ and } \begin{bmatrix} A(s^*) - (\nu(s^*) \pm i\omega(s^*))\ \mathrm{I} \\ d^T \end{bmatrix}$$

have full rank. Note that this implies that there exists a unique $e(s) \in E(s)$ with $c^T e(s) = 1$, $d^T e(s) = 0$ for $s \approx s^*$. Furthermore assume that $a, b \in \mathbb{R}^n$ are chosen so that

$$[\, A(s^*)^2 - 2\nu(s^*)A(s^*) + \mathrm{I} \quad a \quad b\,] \text{ and } [\, A(s^*)^2 - 2\nu(s^*)A(s^*) + \mathrm{I} \quad a \quad A(s^*)e(s^*)\,]$$

have full rank. Then the bordered matrix in the linear system

$$\begin{bmatrix} A(s)^2 - 2\mu A(s) + \mathrm{I} & a & b \\ c^T & 0 & 0 \\ d^T & 0 & 0 \end{bmatrix} \begin{bmatrix} \xi(\mu, s) \\ \alpha(\mu, s) \\ \beta(\mu, s) \end{bmatrix} = \begin{bmatrix} 0 \\ 1 \\ 0 \end{bmatrix} \tag{14}$$

is non-singular for $s \approx s^*$ and $\mu \approx \nu(s^*)$. Hence

$$\begin{bmatrix} \xi(\mu, s) \\ \alpha(\mu, s) \\ \beta(\mu, s) \end{bmatrix}$$

is well-defined. Furthermore, the following holds:

1. $$\begin{bmatrix} \xi(\nu(s^*), s^*) \\ \alpha(\nu(s^*), s^*) \\ \beta(\nu(s^*), s^*) \end{bmatrix} = \begin{bmatrix} e(s^*) \\ 0 \\ 0 \end{bmatrix}.$$
2. *$\partial_1 \beta(\nu(s^*), s^*) \neq 0$, hence by the implicit function theorem the equation $\beta(\mu, s) = 0$ defines a parametrization $\mu(s)$ for $s \approx s^*$ such that $\beta(\mu(s), s) = 0$ and $\mu(s^*) = \nu(s^*)$.*
3. *$\tau(s) := \alpha(\mu(s), s)$ has a simple zero at $s = s^*$ and can hence be used as a test function for torus bifurcation.*

PROOF. The non-singularity of the linear system is an immediate consequence of the assumptions on a, b, c, d and that the complex eigenvalue $\nu(s^*) + i\omega(s^*)$ is simple.

1. The first claim follows from the uniqueness of the solution and the definition of $e(s)$.
2. Differentiating the linear system with respect to μ gives

$$\begin{bmatrix} -2A(s) & 0 & 0 \\ 0 & 0 & 0 \\ 0 & 0 & 0 \end{bmatrix} \begin{bmatrix} \xi(\mu,s) \\ \alpha(\mu,s) \\ \beta(\mu,s) \end{bmatrix} + \begin{bmatrix} A(s)^2 - 2\mu A(s) + \mathrm{I} & a & b \\ c^T & 0 & 0 \\ d^T & 0 & 0 \end{bmatrix} \begin{bmatrix} \partial_1\xi(\mu,s) \\ \partial_1\alpha(\mu,s) \\ \partial_1\beta(\mu,s) \end{bmatrix} = \begin{bmatrix} 0 \\ 0 \\ 0 \end{bmatrix}$$

Now we use Cramer's Rule to obtain that

$$\partial_1\beta(\nu(s^*),s^*) = \frac{\det \begin{bmatrix} A(s^*)^2 - 2\nu(s^*)A(s^*) + \mathrm{I} & a & 2A(s^*)\xi(\nu(s^*),s^*) \\ c^T & 0 & 0 \\ d^T & 0 & 0 \end{bmatrix}}{\det \begin{bmatrix} A(s^*)^2 - 2\nu(s^*)A(s^*) + \mathrm{I} & a & b \\ c^T & 0 & 0 \\ d^T & 0 & 0 \end{bmatrix}} \neq 0$$

because of the assumptions on a, b, c, d and since $A(s^*)\xi(\nu(s^*), s^*) = A(s^*)e(s^*) \neq 0$.

3. First we show that

$$\det \begin{bmatrix} \partial_1\alpha(\nu(s^*),s^*) & \partial_2\alpha(\nu(s^*),s^*) \\ \partial_1\beta(\nu(s^*),s^*) & \partial_2\beta(\nu(s^*),s^*) \end{bmatrix} \neq 0 \,. \tag{15}$$

For this purpose we write

$$A^2(s) - 2\mu A(s) + \mathrm{I} = \underbrace{(A(s) - (\mu - i\sqrt{1-\mu^2})\ \mathrm{I})}_{=:\,A_1(\mu,s)} \underbrace{(A(s) - (\mu + i\sqrt{1-\mu^2})\ \mathrm{I})}_{=:\,A_2(\mu,s)}$$

We will also make use of three lemmas which we list after this proof. According to [3, Proposition 1.1] we have to show two things to obtain (15):

(a) $A_1(\mu,s)v \succ v$ and $A_2(\mu,s)v \succ v$ uniformly in $(\mu\,,\,s) \approx (\nu(s^*)\,,\,s^*)$ for $v^T d = 0$. This is a fairly standard consequence of the fact that $\mu(s^*) + i\omega(s^*)$ is a simple eigenvalue of $A(s^*)$ and of the assumptions on d, see Lemma 19 for more details.

(b)

$$\sigma_{n-1}(A^2(s) - 2\mu A(s) + \ \mathrm{I}) \succ |s| + |\mu - \nu(s^*)| \tag{16}$$

Here $\sigma_1(B) \geq \sigma_2(B) \geq \ldots \sigma_n(B) \geq 0$ denote the singular values of a matrix $B \in \mathbb{R}^{n\times n}$. To prove (16), we first use Lemma 17 to obtain

$$\sigma_n(A(s) - (\mu + i\sqrt{1-\mu^2})\ \mathrm{I}) \succ (\mu - \nu(s)) + i(\sqrt{1-\mu^2} - \omega(s))\ .$$

We want to use Lemma 18 with

$$k(\mu,s) := \begin{bmatrix} \mu - \nu(s) \\ \sqrt{1-\mu^2} - \omega(s) \end{bmatrix}$$

and calculate the Jacobian:

$$k'(\nu(s^*),s^*) = \begin{bmatrix} 1 & -\nu'(s^*) \\ -\nu(s^*)/\omega(s^*) & -\omega'(s^*) \end{bmatrix}.$$

We obtain

$$\det k'(\nu(s^*),s^*) = \omega(s^*)^{-1}(-\omega'(s^*)\omega(s^*) - \nu'(s^*)\nu(s^*)) \neq 0\ .$$

Here we used the fact that $\nu^2(s) + \omega^2(s) - 1$ has a simple zero at $s = s^*$ and thus the derivative $2\nu(s^*)\nu'(s^*) + 2\omega(s^*)\omega'(s^*) \neq 0$. Hence, by using Lemma 18, we can continue our above estimate to conclude

$$\sigma_n(A_2(\mu,s)) = \sigma_n(A(s) - (\mu + i\sqrt{1-\mu^2})\ \mathrm{I}) \succ |s| + |\mu - \nu(s^*)|\ .$$

Combining this with the fact that

$$\sigma_{n-1}(A_1(\mu,s)) = \sigma_{n-1}(A(s) - (\mu - i\sqrt{1-\mu^2})\ \mathrm{I}) \succ 1$$

for $[s,\mu] \approx [0,\nu(s^*)]$, we now obtain from $\sigma_{n-1}(A_1A_2) \geq \sigma_{n-1}(A_1)\,\sigma_n(A_2)$ the nondegeneracy condition (16).
We have established (15) and use this in the following way. Let us define $\tilde{\alpha}(s) := \alpha(\mu(s),s)$. We know that $\tilde{\alpha}(s^*) = 0$ and have to show that $\tilde{\alpha}'(s^*) \neq 0$. We have

$$\tilde{\alpha}'(s^*) = \partial_1\alpha(\nu(s^*),s^*)\,\mu'(s^*) + \partial_2\alpha(\nu(s^*),s^*)\ .$$

From $\beta(\mu(s), s) = 0$ we obtain

$$0 = \partial_1\beta(\nu(s^*), s^*)\,\mu'(s^*) + \partial_2\beta(\nu(s^*), s^*)\ .$$

Note that $\partial_1\beta(\nu(s^*), s^*) \neq 0$ was already established. Eliminating $\mu'(s^*)$ in the last two equations leads to

$$\tilde{\alpha}'(s^*) = \partial_2\alpha(\nu(s^*), s^*) - \partial_1\alpha(\nu(s^*), s^*)\,\frac{\partial_2\beta(\nu(s^*), s^*)}{\partial_1\beta(\nu(s^*), s^*)}$$

which is different from zero because of (15). □

The previous proof used the following lemmas:

LEMMA 17. *Let $s \in \mathbb{R} \mapsto B(s) \in \mathbb{R}^{n\times n}$ and $s \in \mathbb{R} \mapsto \rho(s) \in \mathbb{C}$ be smooth and such that $\rho(s)$ is an eigenvalue of $B(s)$ and $\rho(s^*)$ is an algebraically simple eigenvalue of $B(s^*)$. Then $\sigma_n(B(s) - \rho(s)\ \mathrm{I}) \succ |\rho(s^*) - \rho(s)|$.*

A proof can be obtained by following arguments in [3, p. 533].
The next lemma is well-known:

LEMMA 18. *If $k : \mathbb{R}^2 \to \mathbb{R}^2$ is smooth, $k(y_0) = 0$, and $k'(y_0)$ non-singular, then $k(y) \succ y - y_0$.*

The following lemma seems to be fairly standard, see, e.g., the techniques used in [6].

LEMMA 19. *Let $B : \mathbb{R}^k \to \mathbb{R}^{m\times m}$ be continuous and such that $B(0)$ has 0 as an algebraically simple eigenvalue. Let $d \in \mathbb{R}^m$ be such that*

$$\begin{bmatrix} B(0) \\ d^T \end{bmatrix}$$

has full rank. Then

$$B(\lambda)v \succ v \text{ for } v \in \mathbb{R}^m \text{ with } v \perp d$$

uniformly for $\lambda \approx 0$.

REMARK 20. Note that the theorem gives a local result. We therefore propose to use it in conjunction with an Arnoldi iteration: While following a branch of periodic solutions, we occasionally apply an Arnoldi-type iteration (we used ARPACK [11]) to obtain snapshots of the dominant eigenvalues (Floquet multipliers) of the monodromy matrix $\partial_1\varphi(u,T,\lambda)$. The snapshot will show when a pair of conjugate complex eigenvalues passes through the unit circle. We then use the above test-function as described in Section 4 to approximate the torus bifurcation point more accurately. Note that the Arnoldi-like method not only gives us guesses for μ via the real part of the approximate eigenvalue, but also choices for a and b via the real and imaginary part of the approximate eigenvector. This proved to be an effective and efficient strategy.

8 – Implementing the action of $H'(u,T,\lambda)$

As has been seen in the preceding sections, in order to perform the predictor-corrector steps of numerical continuation and the evaluation of the test functions for bifurcations, it is necessary to implement the action of the Jacobian $H'(u,T,\lambda) = \begin{bmatrix} \partial_1\varphi - I & \partial_2\varphi & \partial_3\varphi \\ \partial_1 h & \partial_2 h & \partial_3 h \end{bmatrix}(u,T,\lambda)$ efficiently, see also [4], [12], [13].

1. The action $v \mapsto \partial_1\varphi(u,T,\lambda)v$ is obtained in the following way: Defining

$$z(t) := \partial_1\varphi(u,t,\lambda)v$$

and differentiating the equations

$$\partial_2\varphi(u,t,\lambda) = f(\varphi(u,t,\lambda),\lambda), \quad \varphi(u,0,\lambda) = u \tag{21}$$

with respect to u leads to the following description: We solve

$$\dot{z} = \partial_1 f(\varphi(u,t,\lambda),\lambda)\, z, \quad z(0) = v \tag{22}$$

and obtain

$$\partial_1\varphi(u,T,\lambda)v = z(T).$$

2. The vector $\partial_3\varphi(u,T,\lambda)$ is obtained in the following way: Defining

$$\xi(t) = \partial_3\varphi(u,t,\lambda)$$

and differentiating the equations (21) with respect to λ leads to the following description:

We solve

$$\dot{\xi} = \partial_1 f(\varphi(u,t,\lambda),\lambda)\,\xi + \partial_2 f(\varphi(u,t,\lambda),\lambda), \quad \xi(0) = 0 \tag{23}$$

and obtain

$$\partial_3\varphi(u,T,\lambda) = \xi(T).$$

3. The vector

$$\partial_2\varphi(u,T,\lambda) = f(\varphi(u,T,\lambda),\lambda) \tag{24}$$

is immediately obtained from (21)

The action of the other derivatives contained in $H'(u,T,\lambda)$ are even more obvious.

9 – The numerical calculation of φ and its derivatives

The previously indicated implementations all rely on an approximation of the orbit

$$t \mapsto \varphi(u,t,\lambda).$$

Our present aim is only to demonstrate the usefulness and applicability of the *matrix-free approach*. We need to approximate the orbit on a grid $t_0 = 0, t_1, \ldots, t_{m-1}, t_m = T$. For simplicity and convenience, we use an equidistant grid $t_i = ih$ in our numerical example, and note that for greater efficiency an adaptive grid must be taken into consideration.

Since we are mainly interested in cases where $\dot{\varphi} = f(\varphi,\lambda)$ is obtained from parabolic PDEs via space discretizations, we concentrate on the case where $\dot{\varphi} = f(\varphi,\lambda)$ is stiff, hence we have to consider the use of an implicit solver for the time steps. The main point here is that we need to solve a nonlinear system for each time step.

For simplicity, in our numerical example we consider the implicit midpoint rule, i.e., we approximate $\varphi(u,t_i,\lambda) \approx \varphi_i$ via

$$\frac{\varphi_i - \varphi_{i-1}}{h} = f\left(\frac{\varphi_i + \varphi_{i-1}}{2}, \lambda\right).$$

We solve this for φ_i using an inexact Newton's method, see, e.g., [9], where the linear equations (per Newton step) are solved with an iterative linear solver (see, e.g., [15]). For a preconditioner we use an (occasionally updated) sparse (possibly incomplete) LU factorization of the approximate Jacobian

$$\mathrm{I} - h\partial_1 f\,(v,\lambda) \;\text{ where } v \approx \varphi_i\ .$$

A few preconditioners are stored along an orbit, and are used again for small variations in u and λ.

The linear differential equation (22) is solved by the same implicit midpoint rule. This leads to the linear systems

$$\left(\mathrm{I}-\frac{h}{2}\partial_1 f\left(\varphi\left(u,\frac{t_{i+1}+t_i}{2},\lambda\right),\lambda\right)\right)z_{i+1}=\left(\mathrm{I}+\frac{h}{2}\partial_1 f\left(\varphi\left(u,\frac{t_{i+1}+t_i}{2},\lambda\right),\lambda\right)\right)z_i$$

which we have to solve for z_{i+1}. Typically we would replace the unknown $\varphi(u,\frac{t_{i+1}+t_i}{2},\lambda)$ with $\frac{\varphi_{i+1}+\varphi_i}{2}$.

The linear differential equation (23) is also solved by the implicit midpoint rule:

$$\left(\mathrm{I}-\frac{h}{2}\partial_1 f\left(\varphi\left(u,\frac{t_{i+1}+t_i}{2},\lambda\right),\lambda\right)\right)\xi_{i+1}=\left(\mathrm{I}+\frac{h}{2}\partial_1 f\left(\varphi\left(u,\frac{t_{i+1}+t_i}{2},\lambda\right),\lambda\right)\right)\xi_i+$$
$$+h\partial_2 f\left(\varphi\left(u,\frac{t_{i+1}+t_i}{2},\lambda\right),\lambda\right)$$

It is convenient to use the same iterative linear solver for all three cases, with the same preconditioner. We finally note that similar remarks would hold if we replaced the implicit midpoint rule with a higher order implicit solver for (21)-(23).

10 – Numerical Example

The Brusselator in one space dimension (z-variable) is modelled by the equations

$$\begin{aligned}\frac{\partial X}{\partial t}&=\frac{D_X}{L^2}\frac{\partial^2 X}{\partial z^2}+X^2Y-(B+1)X+A,\\ \frac{\partial Y}{\partial t}&=\frac{D_Y}{L^2}\frac{\partial^2 Y}{\partial z^2}-X^2Y+BX\end{aligned}\tag{25}$$

with Dirichlet boundary conditions

$$\begin{aligned}X(t,\,z=0)&=X(t,\,z=1)=A,\\ Y(t,\,z=0)&=Y(t,\,z=1)=B/A,\end{aligned}\tag{26}$$

see, e.g., [7]. As in [12], we use the characteristic length L as the bifurcation parameter while the other parameters are fixed at $A=2$, $B=5.45$, $D_X=0.008$ and $D_Y=0.004$.

It is known, see [12], that the first bifurcation from the trivial solution $X \equiv A$, $Y \equiv B/A$ is a Hopf bifurcation at $L \approx 0.513$ and the bifurcating branch of periodic orbits has two torus bifurcation points between 1.7 and 1.9.

Using a numerical continuation method as described in Section 3, we reconfirmed the bifurcation diagram published in [12].

As an example, we used our torus test function described in Theorem 13 together with the approach described in Section 4 to calculate the two torus bifurcation points more accurately. For this purpose, we chose $m = 100$ time steps to discretize the periodic orbit as described in Section 8. In the space coordinate z we used a central difference discretization with n (equidistant) interior points.

We note that this example is simple in that the solutions are known to be smooth. In fact, for more precise approximations, it would be adequate to use higher order discretizations in space and time. Also, in general, our approach should be modified to allow for adaptive meshes, in particular with respect to time.

However, here we just want to make the point that our matrix-free numerical approach is capable of handling large structures involving a variety of singularities. More complex approaches involving adaptive meshes and/or higher orders are currently under investigation.

For the first torus bifurcation we obtained

n	L
50	1.778310
100	1.783406
200	1.784757

For the second torus bifurcation we obtained

n	L
50	1.864434
100	1.872761
200	1.874973

This data supports the claim that the approximation is quadratic in the space discretization (neglecting the time discretization which was held fixed).
Now we consider the Brusselator in two space dimensions (x and y-coordinates)

$$\frac{\partial X}{\partial t} = \frac{D_X}{L^2}\left(\frac{\partial^2 X}{\partial x^2} + \frac{\partial^2 X}{\partial y^2}\right) + X^2 Y - (B+1)X + A,$$

$$\frac{\partial Y}{\partial t} = \frac{D_Y}{L^2}\left(\frac{\partial^2 Y}{\partial x^2} + \frac{\partial^2 Y}{\partial y^2}\right) - X^2 Y + BX$$

on the unit square $[0,1] \times [0,1]$ with the Dirichlet boundary conditions corresponding to (26) on all boundaries.

Fixing the same parameter values as above, the first branch of periodic orbits bifurcates from the trivial solution at $L \approx 0.72$.

This branch has been computed in [14] for similar parameter values. As in [14], we continued that branch and detected a torus bifurcation point at $L \approx 1.48$, see Figure 1 and Figure 2. We again used our torus test function described in Theorem 13 together with the approach described in Section 9 to precisely calculate this torus bifurcation point.

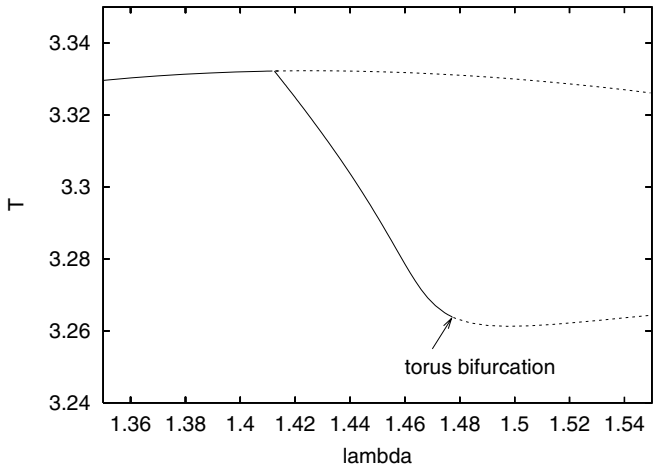

Fig. 1: The numerical continuation for a 20×20 space discretization.

For this purpose, we again chose $m = 100$ time steps to discretize the periodic orbit as described in Section 8. In the space co-ordinates x, y we used a central difference discretization with $n \times n$ (equidistant) interior points.

Note that the resulting computations are already relatively large for direct methods (i.e., generating the monodromy matrix). With our matrix-free approach, however, we were able to perform the required calculations for $n = 40$ on a 600MHz laptop.

The numerical continuation method and the evaluation of the test function have as the main computational expense the time integrations described in Section 9. The stiff solver used there makes use of an iterative linear solver which needs to be preconditioned. We chose some time points on the orbit to generate a sparse LU-factorization of the linear problem, and we used this LU-factorization as a preconditioner for neighboring times, and also for similar parameter val-

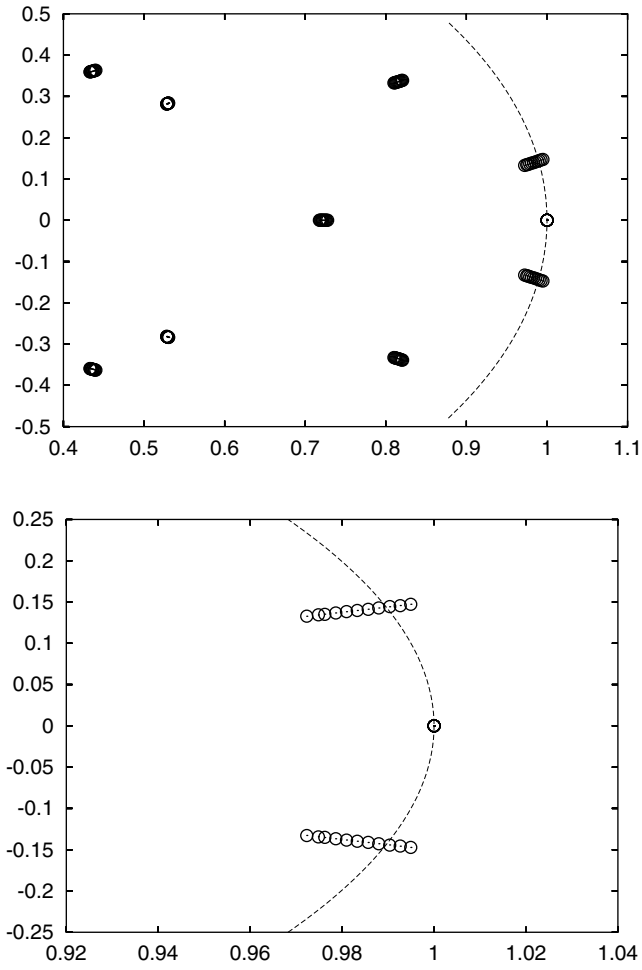

Fig. 2: The trajectories of the 10 eigenvalues with largest magnitude on the λ-interval $[1.47639, 1.48032]$ for a 40×40 space discretization.

ues during the continuation procedure. For finer space discretizations we would propose to use only incomplete LU-factorizations.

For the torus bifurcation we obtained

grid	L
10×10	1.47224
20×20	1.47756
40×40	1.47930

This data again supports the claim that the approximation is quadratic in the space discretization (neglecting the time discretization which was held fixed). Additional efficiencies could be effected by incorporating higher order spatial discretizations and variable time steps.

REFERENCES

[1] E. L. Allgower – K. Georg: *Numerical path following*, In P. G. Ciarlet and J. L. Lions, editors, *Handbook of Numerical Analysis*, volume 5, North-Holland, 1997, pp. 3-207.

[2] R. P. Brent: *Algorithms for minimization without derivatives*, Prentice-Hall Inc., Englewood Cliffs, N.J., 1973. Prentice-Hall Series in Automatic Computation.

[3] K.-W. E. Chu – W. Govaerts – A. Spence: *Matrices with rank deficiency two in eigenvalue problems and dynamical systems*, SIAM J. Num.Anal., **3** (1994), 524-539.

[4] U. Garbotz: *Homokline Orbits in großen Systemen. Ein numerisches Verfahren für Mehrparameter-Probleme*, PhD thesis, University of Marburg, Department of Mathematics, 2001. http://archiv.ub.uni-marburg.de/diss/z2001/0274/.

[5] K. Georg: *Matrix-free numerical continuation and bifurcation*, Numerical Functional Analysis and Optimization, **22** (2001), 303-320.

[6] W. Govaerts: *Numerical Methods for Bifurcations of Dynamical Equilibria*, SIAM, 2000.

[7] M. Holodniok – P. Knedlík – M. Kubíček: *Continuation of periodic solutions in parabolic partial differential equations*, In T. Küpper, R. Seydel, and H. Troger, editors, *Bifurcations: Analysis, Algorithms, Applications*, volume 79 of ISNM, Birkhäuser Verlag, Basel, 1987, pp. 122-130.

[8] H. B. Keller: *Numerical solution of bifurcation and nonlinear eigenvalue problems*, In P. H. Rabinowitz, editor, *Applications of Bifurcation Theory*, Academic Press, New York, London, 1977, pp. 359-384.

[9] C. T. Kelley: *Iterative Methods for Linear and Nonlinear Equations*, SIAM, Philadelphia, 1995.

[10] Yu. A. Kuznetsov.: *Elements of Applied Bifurcation Theory*, volume 112 of Appl. Math. Sci. Springer, second edition, 1998.

[11] R.B. Lehoucq – D.C. Sorensen – C. Yang: *ARPACK Users' Guide*, Software, Environments, Tools. Society for Industrial and Applied Mathematics, 1998.

[12] K. Lust – D. Roose: *Computation and bifurcation analysis of periodic solutions of large-scale systems*, In E. Doedel and L.S. Tuckerman, editors, *Numerical Methods for Bifurcation Problems and Large-Scale Dynamical Systems*. Springer-Verlag, 2000.

[13] K. Lust – D. Roose – A. Spence – A. R. Champneys: *An adaptive Newton-Picard algorithm with subspace iteration for computing periodic solutions*, SIAM Journal on Scientific Computing, **19** (1998), 1188-1209.

[14] D. Roose – S. Vandewalle: *Efficient parallel computation of periodic solutions of partial differential equations*, In R. Seydel and H. Troger, editors, *Bifurcations and Chaos: Analysis, Algorithms, Applications*, ISNM, Birkhäuser Verlag, Basel, 1991, pp. 278-288

[15] Y. Saad: *Iterative Methods for Sparse Linear Systems*, PWS Publishing Company, 1996.

[16] R. Seydel: *From Equilibrium to Chaos. Practical Bifurcation and Stability Analysis*, Elsevier, New York, 1988.

[17] B. Werner: *Computation of Hopf bifurcation with bordered matrices*, SIAM J. Numer. Anal., **33** (1996), 435-455.

Lavoro pervenuto alla redazione il 15 febbraio 2003
ed accettato per la pubblicazione il 21 aprile 2004.
Bozze licenziate il 14 febbraio 2005

Indirizzo degli Autori:

Eugene Allgower, Ulf Garbotz – Department of Mathematics – Colorado State University – Fort Collins, CO 80523
E-mail: allgower@math.colostate.edu ulf@garbotz.de

Work partially supported by NSF via grant # DMS-9870274.